High-throughput Neurotechnology and Quantum Electron Microscopy

1. High-throughput On-chip Small-animal Screening

Sponsors
NIH Director's New Innovator Award
NSERC Postdoctoral Fellowship
Merck-CSBi Graduate Fellowship
NSF Graduate Research Fellowship

Project Staff
Christopher Rohde, Chrysanthi Samara, Cody Gilleland

Overview

Therapeutic treatment of central nervous system pathologies, such as spinal cord injuries, brain trauma, stroke, and neurodegenerative disorders, will greatly benefit from the discovery of small molecules that enhance neuronal growth after injury. Identification of a diverse repertoire of such molecules and of their cellular targets can also provide important tools for fundamental investigations of the mechanisms involved in the regeneration process. Currently, small-molecule screens for factors affecting neuronal regrowth can only be performed using simple in vitro cell culture systems. However, these systems do not truly represent *in vivo* environment. Importantly, off-target, toxic or lethal effects of chemical compounds may only manifest *in vivo*. Thus, the thorough investigation of neuronal regeneration mechanisms requires *in vivo* neuronal injury models.

The size and complexity of the instrumentation used to study large vertebrate animal models prohibits their use in high-throughput assays for rapid identification of new genes and drug targets. Because of this, researchers turn to simpler organisms, and the advantages of using small invertebrate animals as model systems for human disease have become increasingly apparent. The nematode Caenorhabditis elegans (*C. elegans*) is a powerful model organism due to a number of useful properties including its small size, optical transparency, rapid developmental cycle and the availability of a wide array of species-specific genetic techniques. However, since the first studies on *C. elegans* in the early 1960s, little has changed in how scientists manipulate this tiny organism by manually picking, sorting, and transferring individual animals. The reliance on manual techniques means that large-scale forward- and reverse-genetic screens can take several months to years to complete. The high-throughput techniques that exist in *C. elegans* require assays to be significantly simplified in order to be even partially automated.

Fortunately, many of the properties that make *C. elegans* a useful model organism also make it well suited to manipulation in microfluidic channels. This has enabled us to create components for an integrated, whole-animal, high-throughput sorting and large-scale screening platform to perform drug and genetic assays with sub-cellular resolution. We have designed microfluidic devices [1][2] from multiple layers of the flexible elastomer poly(dimethyl siloxane) [3] that can be combined in various configurations to allow a multitude of complex high-throughput assays such as mutagenesis, drug and RNAi screens. These devices are: (i) a small-animal sorter that enables highly-stable of immobilization live, unanesthetized animals; (ii) an array of microfluidic chambers for simultaneous incubation, immobilization, sub-celluar-resolution imaging and independent screening of many animals on a single chip; and (iii) a microfluidic interface to large-scale multiwell-format libraries that also functions as a multiplexed animal dispenser.

The rapid and repeatable animal immobilization which the devices enable allows high-throughput and precise surgery. Following surgery, animals are exposed to the contents of a small-molecule library and assayed for neuronal regeneration. Using this screening method we have identified several compounds that appear to enhance neural regeneration *in vivo*.

Technology Background

On-chip high-throughput immobilization and sorting

The high mobility of *C. elegans* requires them to be immobilized in order to examine cellular and sub-cellular features. This is most commonly done using anesthesia such as sodium azide (NaN_3), levamisole, or tricaine/tetrimisole. However, anesthetics can have negative or uncharacterized side-effects on biological processes. Cooling can also be used to reversibly immobilize animals, however this can also have unpredictable effects, especially since many *C. elegans* strains are especially sensitive to temperature variations. Additionally, these immobilization techniques are not suitable for assays requiring physiologically active animals, such as investigations into germ-line proliferation, development, or neurophysiology.

We have developed a microfluidic small-animal sorter that can rapidly isolate and immobilize individual animals. The sorter consists of control channels and valves (gray) that direct the flow of worms in the flow channels in different directions (Figure 1) [1]. A worm is captured in the chamber by suction via the top channel while the lower suction channels are inactive. The chamber is then washed to flush any other worms in the chamber (blue line) toward the waste or back to the circulating input. The chamber is isolated from all of the channels and the worm is released from the top suction channel to be restrained by the lower suction channels (red line). The aspiration immobilizes animals only partially, and it is not sufficient to completely restrict their motion. In order to fully immobilize the animals, we create a seal around them that restricts their motion completely. This is done by using a 15–25 μm-thick flexible sealing membrane that separates a press-down channel from the flow channel below (Figure 1e) [2]. The press-down channel can be rapidly pressurized to expand the thin membrane downwards, wrapping around the animals and forming a tight seal which completely constrains their motion in a linear orientation. The image acquisition and processing are then performed, and the worm is either collected or directed to the waste, depending on its phenotype. Quantitative analysis of the immobilization stability shows that it is comparable to chemical anesthetics, and there was no change in the lifespan or brood size of the immobilized animals [2]. Additionally, visual observation of the animals and their neurons showed no signs of hypoxia or other distress.

Following immobilization, the worm can be imaged at sub-cellular resolution using high-resolution optics. The stability achieved is sufficient to allow three-dimensional imaging and sub-cellular manipulation using femotosecond laser micro-surgery (see below). Following phenotype identification the captured animal is released and can be directed to one of two collection channels.

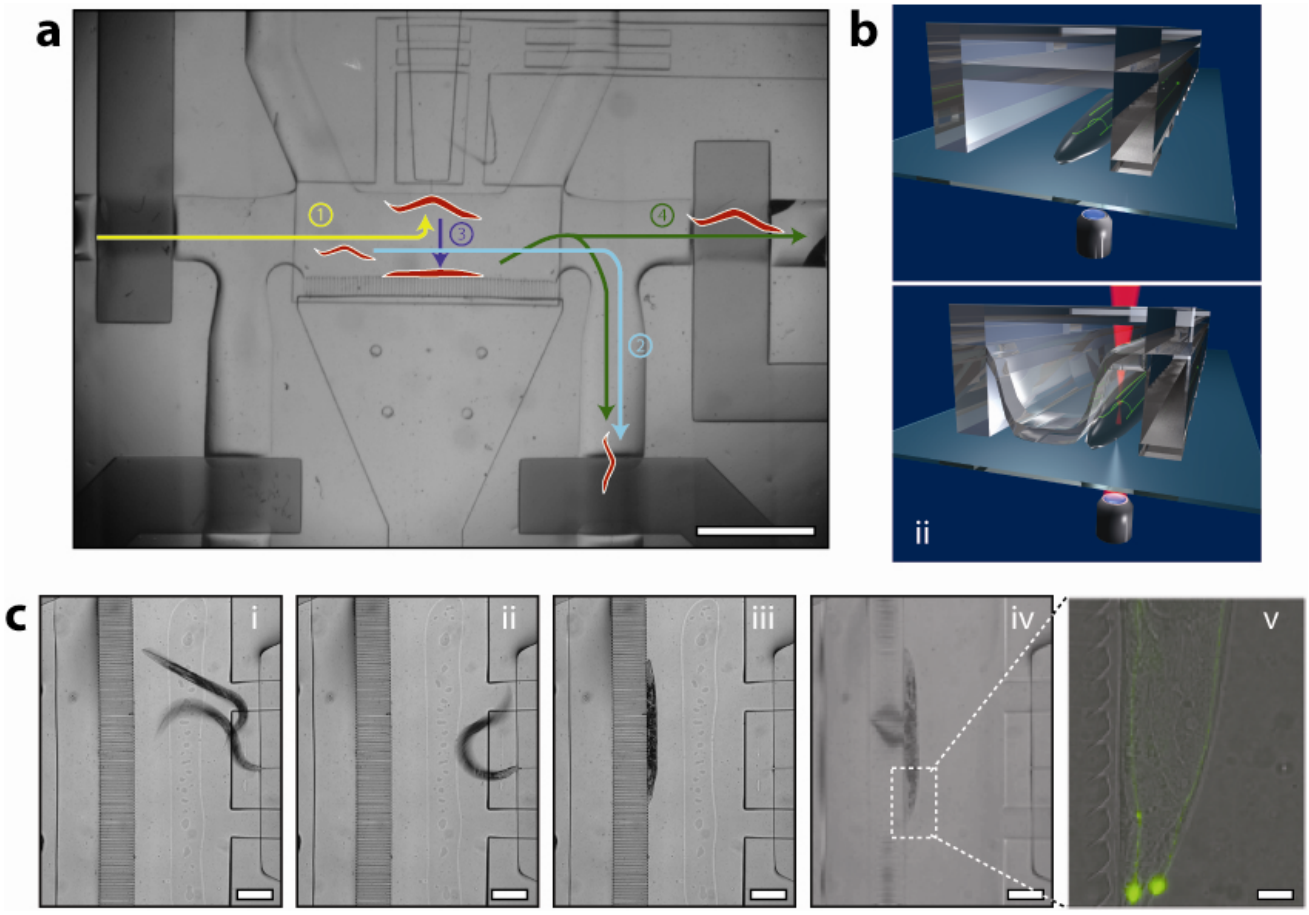

Figure 1. Microfluidic immobilization for femtosecond laser surgery of C. elegans. (a) Micrograph of chip with numbered arrows showing microfluidic C. elegans manipulation steps. 1: Loading of nematodes and capture of a single animal by one aspiration channel. 2: Washing of the channels to remove and recycle the rest of the nematodes. 3: Release of the captured animal from single aspiration port, and recapture and orientation of it by a linear array of aspiration ports. 4: Collection of the animal after surgery. Scale bar: 1 mm. (b) Illustration of the final immobilization and laser axotomy: Once a single animal is captured and linearly oriented (i), a channel above it is pressurized pushing a thin membrane downwards (ii). This membrane wraps around the animal significantly increasing immobilization stability for imaging and surgery. (c) Single animal capture (i), isolation (ii) and immobilization (iii & iv). (v) shows combination bright-field of animal and fluorescent image of gfp-labeled posterior lateral mechanosensory neurons. Scale bars: (i)-(iv) 250 μm, (v) 20 μm.

Large-Scale Time-Lapse Studies Using Multiplexed Incubation chambers

High-throughput time-lapse studies on small animals are currently performed in multiwell plates by automated fluorescence microplate readers [4]. Because the animals swim inside the wells, only average fluorescence is obtained from each well, and cellular and sub-celluar details cannot be imaged. Although anesthesia can be used to immobilize the animals, the effects of long-term anesthesia prohibit many time-lapse screeens, and anesthesia has detrimental effects on many biological processes. Additionally, animal loss can occur during media exchange. To address these problems, we designed the microfluidic-chamber device shown in Figure 2(a) for worm incubation and for continuous imaging at sub-celluar

resolution. Sorted worms can be delivered to the chambers by opening valves via multiplexed control lines [5].

Microchamber chips based on this design can be readily scaled for large-scale screening applications because the number of control lines required to independently address *n* incubation chambers scales only with log(n) [5]. The millimeter scale of the microchambers can allow hundreds of microchambers to be integrated on a single chip. To image animals, a flow is used to push the animals toward the posts arranged in an arc inside the chambers (Figures 2(b) and 2(c)). This flow restrains the animals for sub-celluar imaging. The arrangement of the posts positions animals in a similar configuration, which simplifies the analysis of images. The medium in the chambers can be exchanged through the microfluidic channels for complex screening strategies, and precisely timed exposures to biochemicals (e.g., drugs/RNAi) can be performed. The use of microfluidic technology also reduces the cost of whole-animal assays by reducing the required volumes of compounds.

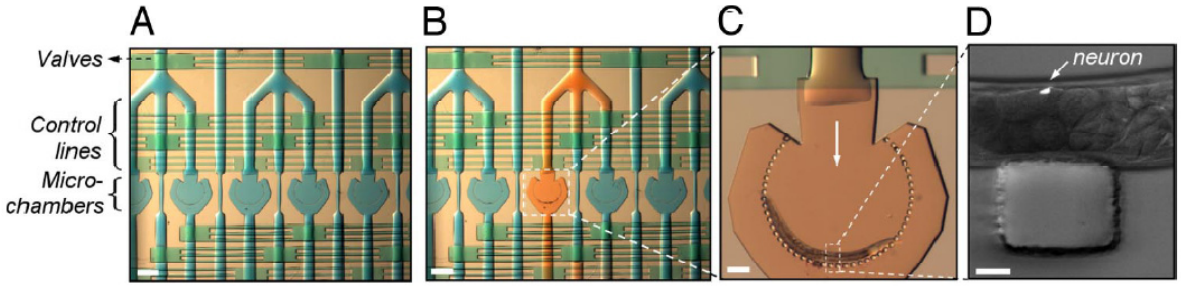

Figure 2. Individually addressable microfluidic screening chambers.

Well-plate interfacing

Interfacing microfluidics to existing large-scale RNAi and drug libraries in standard multiwell plates represents a significant challenge as it is impractical to deliver compounds to hundreds of microchambers on a single chip through hundreds of external fluidic connectors. The interface device in Figure 3 addresses this problem. This microfluidic interface chip consists of an array of aspiration tips that can be lowered into the wells of microwell plates, which allows minute amounts of library compounds to be collected from the wells by suction, routed through multiplexed flow lines one at a time, and delivered to the single output of the device. Following delivery the lines of the chip can be easily and automatically washed to prevent cross-contamination. The output of the interface chip can then be connected to our microfluidic-chamber device for sequential delivery of compounds to each microchamber. Combining this multiwell-plate interface chip with existing robotic multiwell-plate handlers will allow large libraries to be delivered to microfluidic chips. The same device can also be used to dispense worms into multiwell plates, simply by running it in reverse.

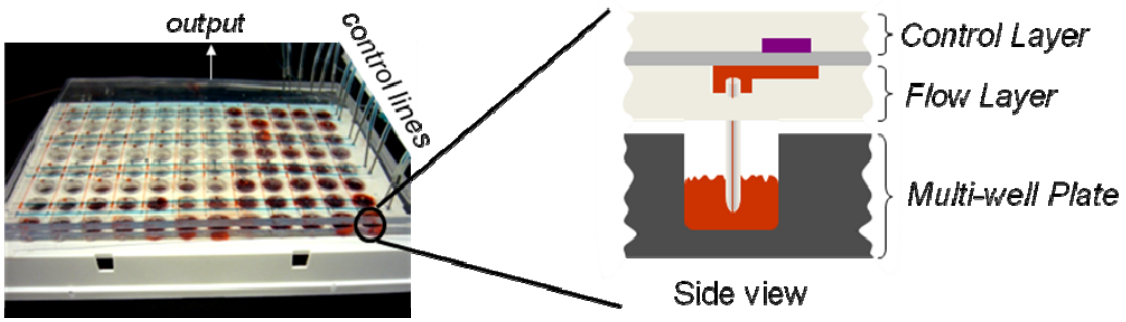

Figure 3: Microfluidic interface device for large-scale compound delivery.

Applications

Femtosecond-laser micro/nanosurgery enables precise ablation of sub-cellular processes with minimal collateral damage [6] and we have previously employed this technique to perform the first axonal regeneration study in *C. elegans* [7][8]. However, manually preparing an animal for surgery, imaging and recovering it afterwards are laborious. Additionally, the effects of long-term anesthesia on biological processes are not known. We can use our immobilization technique to repeatably and rapidly immobilize animals and perform femtosecond-laser microsurgery with sub-cellular precision.

Another application requiring an even higher degree of stabilization is multi-photon microscopy [9]. This technique has the ability to perform optical sectioning with negligible out-of-plane absorption and emission due to its non-linearity. This dramatically reduces photobleaching and phototoxicity, [10] which is especially significant in assays that require animals to be imaged at multiple time points. Both of these applications are illustrated in Fig 4.

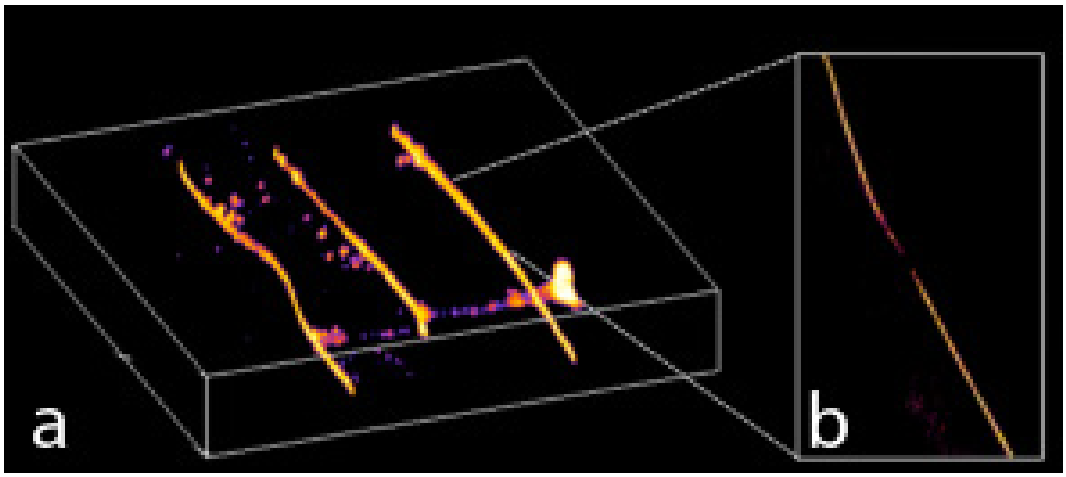

Figure 4. On-chip small-animal immobilization allows for the use of many powerful optical techniques. Both (a) three-dimensional two-photon imaging and (b) femtosecond laser microsurgery can be rapidly and repeatedly performed on chip.

Screening for Factors Affecting Neural Regeneration

The speed and accuracy of immobilization achieved by our microfluidic devices enables large-scale screening of chemical and genetic libraries. We have used these devices to screen for compounds

affecting neural regeneration following axotomy. Animals were subsequently exposed to elements of a small-molecule library containing a wide variety of compounds. By analyzing the length of regenerating axons following compound exposure, we identified several compounds that enhance neuronal regeneration *in vivo* (Figure 5). By performing various RNAi screens using these laser and microfluidic technologies, we also identified genetic targets of these compounds.

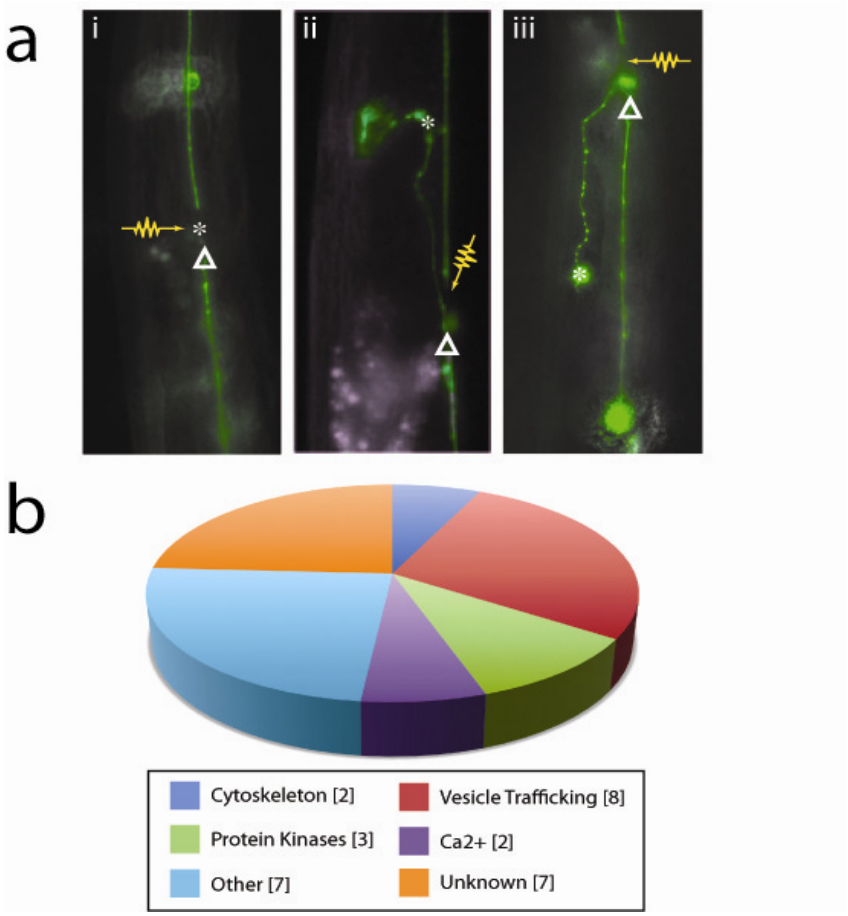

Figure 5. (a) Illustration of some regeneration types observed following laser surgery and compound exposure. i) Short regeneration in control animal. ii,iii) Long regeneration in the presence of compound. Arrow indicates original surgery location, triangles (Δ).

References

[1] C. B. Rohde, F. Zeng, R. Gonzalez-Rubio, M. Angel, M. F. Yanik: PNAS, 104, (2007) 13891.

[2] F. Zeng, C. B. Rohde, M. F. Yanik, Lab Chip, 8 (2008) 653.

[3] D. C. Duffy, J. C. McDonald, O. J. A. Schueller and G. Whitesides: Anal. Chem., 70, (1998) 4974.

[4] Kaletta T, Butler L, Bogaert T (2003) Model Organisms in Drug Discovery (Wiley, West Sussex, UK).

[5] J. Melin and S. Quake: Annu Rev Biophys Biomol Struct, 36, (2007) 213.

[6] A. Vogel, J. Noack, G. Huttman and G. Paltauf: Appl. Phys. B: Lasers Opt., 81, (2005) 1015.

[7] M. F. Yanik, H. Cinar, H. N. Cinar, A. D. Chisholm, Y. Jin and A. Ben-Yakar: Nature, 432, (2004) 822.

[8] M. F. Yanik, H. Cinar, H. N. Cinar, A. Gibby, A. D. Chisholm, Y. Jin and A. Ben-Yakar: IEEE J. Sel. Top. Quantum Electron., 12, (2006) 1283.

[9] W. Denk, J. H. Strickler and W. W. Webb: Science, 248, (1990) 73.

[10] G. Filippidis, C. Kouloumentas, G. Voglis, F. Zacharopoulou, T. G. Papazoglou and N. Tavernarakis: J. Biomed. Opt., 10, (2005) 024015

2. Noninvasive Quantum Electron Microscopy

Sponsors
David and Lucille Packard Foundation

Project Staff
William Putnam

Overview

Electron microscopy has significantly impacted many areas of science and engineering due to its unprecedented atomic and molecular resolution. Yet, the imaging of biological and other sensitive specimens has been limited because of the sample damage induced by the energetic electrons necessary for imaging. For example, the radiation dose received by a specimen during imaging with a transmission electron microscope operating under typical conditions is comparable to the radiation exposure from a ten megaton hydrogen bomb exploded about thirty meters away [1]. Nobel Laureate Dennis Gabor, who investigated several electron microscopy techniques, concluded in his famous review [2]: “The fundamental limitation of electron interferometers… is the destruction of the object by the exploring agent, and in this respect electron interferometers appear to be neither better nor worse than other instruments.” Despite progress in hydrated environmental chambers for viewing biological specimens in their native state [3,4], when exposed to such energetic electrons, sensitive specimens experience substantial mass loss, modification of chemical bonding, or other structural damage [3,5].

We have proposed the use of interaction-free quantum measurements with electrons to eliminate sample damage in electron microscopy. The application of such a quantum electron microscopy (QEM) technique might allow noninvasive molecular-resolution imaging. We have demonstrated the theoretical possibility of such measurements in the presence of experimentally measured quantum decoherence rates and using an arrangement based on existing charged particle trapping techniques [6].

Technology Background and Research

At first sight, one might conclude that any measurement requires physical interaction with the measured object. Yet, it has been shown that a non-transmitting object in the arm of an optical interferometer can modify the interference of a single photon in such a way that the presence of the object can be detected without interaction (i.e., energy exchange) between the photon and the object [7,8,9,10,11]. Such interaction-free measurements have been employed in optical microscopy with photons [12] but have never previously been considered with electrons.

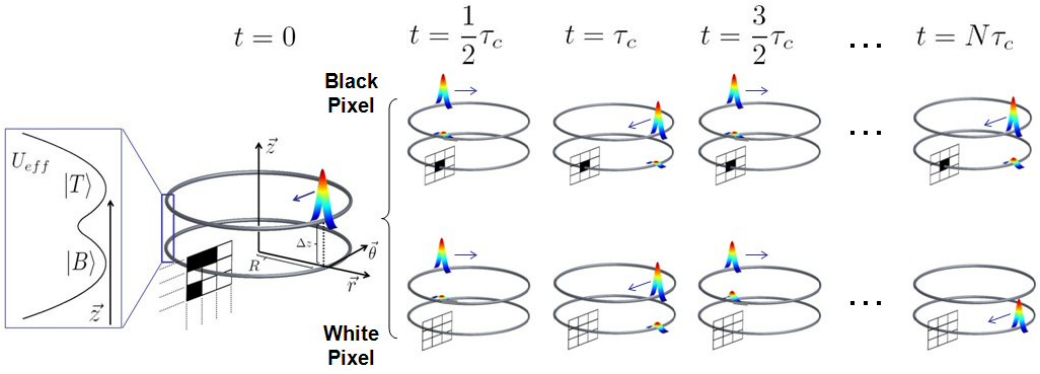

Figure 1: Interaction-free imaging with electrons

Interaction-free imaging with electrons can fundamentally be understood from the illustration in Figure 1. Two ring shaped electron traps are vertically stacked as drawn in Figure 1. The ring traps guide electron wavepackets (colorfully drawn in Figure 1) around circular trajectories as shown. The ring traps' potential also couples the two rings creating a double-well potential (pictorially represented in inset). The grid in the lower ring is the object being imaged, which is composed of opaque and transparent regions (i.e. black and white pixels). With a transparent region, the electron tunneling between the two coupled ring traps is uninhibited and after some number of circulations around the rings the electron completely transfers to the lower ring (in Figure 1, τ_C refers to the time required for an electron to circulate about a ring). An opaque region, on the other hand, repeatedly interrupts this tunneling, and the electron remains with high probability in the top ring. This is just a discrete Quantum Zeno effect. Therefore, measurement of an electron's location (in the top or bottom ring) at a specified time can distinguish between the presence of an opaque or transparent region (black or white pixel) without interacting with the object.

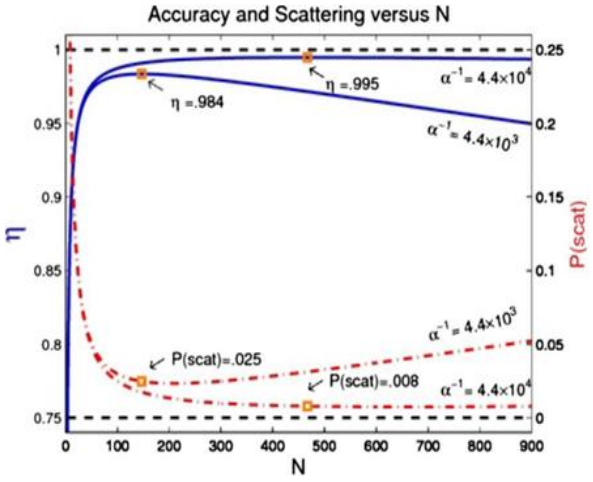

Figure 2: Accuracy and scattering with environment

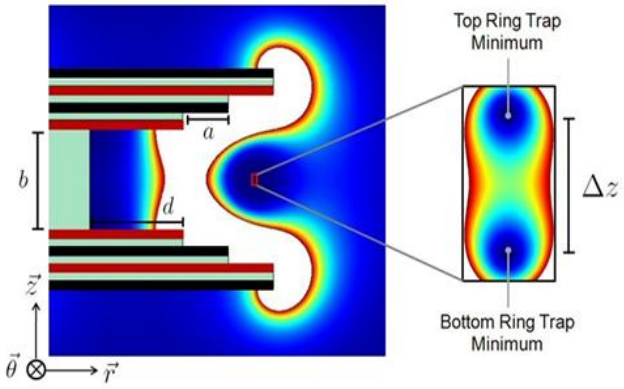

Figure 3: Possible ring trap implementation

Interactions with image charges and fluctuating noise fields in the surrounding environment decohere trapped electrons and limit the accuracy of interaction-free imaging. As electrons move in the ring traps, they induce image charges on the trap electrodes. The image charge distributions constitute *which path* information and result in the decoherence of the electron's spatial state to an incoherent mixture. Using

open-quantum systems techniques, the effect of decoherence on the accuracy and efficiency (or scattering) of our interaction-free measurement system can be estimated and is drawn in Figure 2 [6]. The blue curves correspond to the accuracy of interaction-free measurement for a trap arrangement with rings of 1 cm and 1 mm, 100 KeV electrons, and a realistic decoherence time of 1.7 μs; they are plotted against the number of times the electron is allowed to circulate the ring traps before measurement. The red curves correspond to the probability of an electron scattering off the object being imaged (same trap/electron parameters as given above). We note that the probability of scattering is equal to the electron exposure reduction as scattering probability is proportional to exposure, so with our scheme, electron exposure can, within reason, be reduced by two orders of magnitude, which could be enough to allow noninvasive imaging of molecular processes such as protein activity [3].

The design of the ring shaped electron traps is another issue we have addressed. Figure 3 shows a drawing of the cross-section of the effective potential of a possible ring trap structure. The structure consists of two surface-electrode Paul traps arranged in a v-type configuration. If the v-type configuration is bent into a circle, two coupled ring traps can be made. Figure 3 actually illustrates a multilayered structure equivalent to the v-type configuration but simpler for fabrication. The detailed physics of this trap structure have been analyzed [6], and the tunneling rate, noise tolerances, and decoherence timescale for a structure of this sort have all been shown to provide a reasonable platform to explore interaction-free measurements with electrons and quantum electron microscopy.

In summary, we have proposed and demonstrated the possibility of noninvasive measurements with electrons even in the presence of worst-case electron decoherence rate estimates using an interaction-free measurement scheme based on charged particle trapping techniques [6]. Interaction-free quantum electron microscopy (QEM) can prevent sample exposure to highly energetic and destructive electrons in electron microscopy, which might allow noninvasive imaging of dynamic processes at molecular resolution and open frontiers in imaging.

References

[1] D. T. Grubb and A. Keller, Proceedings of the Fifth European Regional Conferences on Electron Microscopy, Manchester, 1972 (unpublished), pp. 554–560.
[2] D. Gabor, Rev. Mod. Phys. **28**, 260 (1956).
[3] A. M. Glauert, J. Cell Biol. **63**, 717 (1974).
[4] S. Thiberge *et al.*, Proc. Natl. Acad. Sci. U.S.A. **101**, 3346 (2004).
[5] R. Glaeser and K. Taylor, J. Microsc. **112**, 127 (1978).
[6] W. P. Putnam and M. F. Yanik, Phys. Rev. A **80**, 040902(R) (2009).
[7] A. Elitzur and L. Vaidman, Found. Phys. **23**, 987 (1993).
[8] P. Kwiat, H. Weinfurter, T. Herzog, A. Zeilinger, and M. A. Kasevich, Phys. Rev. Lett. **74**, 4763 (1995).
[9] T. Tsegaye *et al.*, Phys. Rev. A **57**, 3987 (1998).
[10] P. G. Kwiat *et al.*, Phys. Rev. Lett. **83**, 4725 (1999).
[11] J. Jang, Phys. Rev. A **59**, 2322 (1999).
[12] A. G. White, J. R. Mitchell, O. Nairz, and P. G. Kwiat, Phys. Rev. A **58**, 605 (1998).